JPET Fast Forward. Published on December 30, 2011 as DOI: 10.1124/jpet.111.189589

JPET#189589

TITLE PAGE

RESVERATROL ATTENUATES DOXORUBICIN-INDUCED CARDIOMYOCYTE DEATH VIA INHIBITION OF S6K1-MEDIATED AUTOPHAGY

Xianmin Xu, Kai Chen, Satoru Kobayashi, Derek Timm, Qiangrong Liang*

All authors are from Cardiovascular Health Research Center, Sanford Research/University of South Dakota, Sioux Falls, South Dakota (X.X., K.C., S.K., D.T., and Q.L.)

Running title: Resveratrol inhibits Doxorubicin cardiotoxicity

Address Correspondence to: Dr. Qiangrong Liang, Cardiovascular Health Research Center, Sanford Research/USD, University of South Dakota Sanford School of Medicine, Sioux Falls, SD 57104. Tel. 605-312-6304; Fax. 605-312-6071; E-mail: Qiangrong.Liang@sanfordhealth.org

Number of text pages: 34

Number of tables: 0

Number of figures: 9

Number of references: 38

Number of words in Abstract: 199

Number of words in Introduction: 553

Number of words in Discussion: 1374

Non standard abbreviations: DOX , doxorubicin; NRC, neonatal rat ventricular cardiomyocyte; h, hour; mTOR, mammalian target of rapamycin; AMPK, AMP-activated protein kinase; PI3K, phosphatidylinositol 3-kinase; DMEM, Dulbecco's modified Eagle's medium; RV, resveratrol; 3-MA, 3-methyladenine; Rap, Rapamycin; BFA, bafilomycin A1; PARP, poly(ADP-ribose) polymerase; siRNA, small interfering RNA; PI, propidium iodide; ANOVA, analysis of variance; shRNA, short hairpin RNA; GAPDH, glyceraldehyde-3-phosphate dehydrogenase; AVs, atophagic vacuoles; GFP, green fluorescent protein. S6K1, p70 ribosomal protein S6 kinase 1; LC3, Microtubule-associated protein light chain 3; Atg, Autophagy-related; BCN1, beclin 1. MOPS, ethylene glycol bis(2 aminoethylether)-N-N' tetra acetic acid. EGTA, morpholinopropane sulfonic acid. DTT, dithiothreitol.

Recommended section assignment: Cadiovascular

ABSTRACT:

Resveratrol is a plant-derived polyphenol that can attenuate the cardiotoxic effects of doxorubicin (DOX), a powerful antibiotic widely used in cancer chemotherapy. However, the underlying protective mechanisms of resveratrol remain elusive. Here we show that resveratrol inhibited DOX-induced autophagy and cardiomyocyte death, and that autophagy suppression is an important mechanism that mediates the ability of resveratrol to protect against DOX cardiotoxicity. Indeed, resveratrol, 3-methyladenine (3-MA) and a short hairpin RNA directed against autophagy gene beclin 1 (shBCN1) each was able to attenuate DOX-induced autophagy and cardiomyocyte death, but resveratrol did not provide additional protection in the presence of 3-MA or shBCN1. In contrast, upregulation of autophagy by beclin 1 overexpression not only exacerbated DOX cardiotoxicity but also abolished the protective effects of resveratrol. Intriguingly, p70 S6 kinase (S6K1) was activated by DOX, which was prevented by resveratrol. Knocking down S6K1 with siRNA diminished DOX-induced autophagy and cardiotoxicity, but resveratrol failed to exert an additive effect. In addition, S6K1 overexpression impaired the ability of resveratrol to antagonize DOX-induced autophagy and cardiomyocyte death. Taken together, our data indicated that the protective effect of resveratrol against DOX cardiotoxicity is largely dependent on its ability to suppress DOX-induced autophagy via inhibition of S6K1.

INTRODUCTION

Doxorubicin (DOX) is a potent anthracycline antibiotic that has been used in anti-cancer therapy for decades. However, DOX is also well known to exert toxic effects on normal tissues. Especially in the heart, DOX can induce a dose dependent cardiomyopathy that ultimately leads to congestive heart failure (Minotti et al., 2004). Despite its severe cardiotoxicity, DOX remains a major component of most chemotherapeutic regimens due to its efficacy and broad-spectrum antitumor activity. As a result, sustained research effort has been devoted to identifying effective drugs or strategies that can reduce DOX cardiotoxicity without compromising its antitumor efficacy.

Resveratrol is a plant-derived polyphenol reported to extend lifespan in lower organisms through mimicking caloric restriction (Wood et al., 2004). As such, resveratrol has been shown to reduce a variety of age-related diseases in rodents, including obesity, diabetes, cancer, cardiovascular diseases, and neurodegenerative diseases (Baur and Sinclair, 2006). Consistently, resveratrol is able to inhibit DOX-induced cardiotoxicity as shown by reduced oxidative stress and improved cardiac function (Tatlidede et al., 2009). Importantly, the cardioprotective effect of resveratrol is associated with enhanced anti-cancer efficacy of DOX in both *in vitro* and *in vivo* studies (Aggarwal et al., 2004; Rezk et al., 2006). This raises the possibility that the combined use of DOX with resveratrol may be a viable chemotherapeutic modality that can selectively destroy tumors while concurrently limiting cardiac damage. However, how resveratrol could achieve these beneficial effects in the setting of DOX chemotherapy remains poorly understood.

DOX-induced oxidative stress has been proposed as the major mechanism responsible for cardiac damage (Minotti et al., 2004), and antioxidant therapies are able to attenuate DOX cardiotoxicity in diverse animal models (Yen et al., 1996; Minotti et al., 2004). Meanwhile, resveratrol has been shown to protect against DOX-induced cardiac dysfunction, mitochondrial depolarization and cardiomyocyte death, which are accompanied by enhanced antioxidant

JPET Fast Forward. Published on December 30, 2011 as DOI: 10.1124/jpet.111.189589
This article has not been copyedited and formatted. The final version may differ from this version.

activity and inhibited production of reactive oxygen species (Tatlidede et al., 2009). These observations suggest that the protective effects of resveratrol against DOX cardiotoxicity may be mediated by its ability to inhibit oxidative stress. Nevertheless, clinical trials demonstrate very limited efficacy of antioxidant supplements in reducing DOX-triggered cardiac injury (Gianni et al., 2008), suggesting that mechanisms other than oxidative stress might also contribute to DOX cardiotoxicity. It is thus possible that resveratrol may exert its cardioprotective effects independent of its inhibitory effects on DOX-induced oxidative stress.

Autophagy is a degradation system for eukaryotic cells to turn over organelles and long-lived proteins thereby maintaining cellular homeostasis. Thus, reduced autophagic activity impairs basal cardiac function and structure (Taneike et al., 2011), making animals more sensitive to stress-induced heart failure (Nakai et al., 2007). However, activation of autophagy could be either beneficial or detrimental to the heart depending on the context. On one hand, autophagy is induced to offset energy deficit promoting myocardial survival in response to starvation (Kuma et al., 2004) or ischemia (Matsui et al., 2007). On the other hand, elevated autophagy can cause cardiac injury under certain conditions. For example, high level autophagy during reperfusion is harmful (Matsui et al., 2007), and diphtheria toxin triggers autophagy leading to heart failure in mice (Akazawa et al., 2004). Similarly, DOX can induce autophagy in cardiomyocytes, which is detrimental in nature since inhibiting autophagy with chemical or genetic approach dramatically attenuates DOX-induced cardiomyocyte death (Lu et al., 2009; Kobayashi et al., 2010; Chen et al., 2011). Thus, a potential therapeutic strategy to reducing DOX cardiotoxicity is to suppress DOX-induced autophagy.

In the present study, we demonstrated that resveratrol markedly reduced DOX-induced cardiomyocyte death, which was largely dependent on its ability to inhibit autophagy. Interestingly, our results also suggested that the inhibition of p70 S6 kinase 1 (S6K1) is essential for resveratrol to suppress DOX-induced autophagy and cytotoxic effects.

MATERIALS AND METHODS:

Cardiomyocyte Cultures. Neonatal rat ventricular cardiomyocytes (NRCs) were cultured as described previously (Kobayashi et al., 2010). Briefly, hearts from 0–2-day-old Harlan Sprague-Dawley rat neonates were dissected and isolated in cold phosphate-buffered saline (PBS), then trypsin was used to dissociate the heart tissues. To prevent cell clumping, DNase was used to digest sticky DNA released from lysed cells. Cells were pre-plated for 1 hour (h) following digestion to remove non-myocytes. Cells were then seeded on gelatinized cell culture dishes overnight in Dulbecco's modified Eagle's medium (DMEM) with 15% bovine serum. Media were changed to DMEM with 2% bovine serum the following day. After being cultured for another 24 h, cells were treated with drugs as indicated. All media contain penicillin and streptomycin (100 units/ml) as well as 100 μM 5-bromo-2′-deoxyuridine (BrdUrd, Sigma) unless otherwise indicated. BrdU was used to inhibit the proliferation of non-myocytes including fibroblasts.

Drug Treatments. Doxorubicin (D1515, DOX), resveratrol (R5010, RV) and 3-methyadenine (M9281, 3-MA) were purchased from Sigma (Saint Louis, MO). Bafilomycin A1 (B1080, BFA) was obtained from LC laboratories (Woburn, MA). DOX was dissolved in saline to make 1mM stock solution and then diluted 1000 times to make a final concentration of 1 μM upon use. Resveratrol was dissolved in ethanol to achieve 10 mM stock solution and was then diluted 1000 times upon use to make a final concentration of 10 μM except for dose response experiments, which was diluted to a series of concentrations. BFA can specifically inhibit vacuolar proton ATPase and efficiently blocks fusion between autophagosomes and lysosomes to prevent maturation of autophagic vacuoles. BFA was dissolved in dimethyl sulfoxide (DMSO) to make a 50 μM stock solution. BFA was added to culture medium 6h before harvesting cells for measuring autophagic flux.

Western Blot Analysis. Protein extraction from cardiomyocytes were performed by following protocol described previously (Kobayashi et al., 2007). Briefly, cultured NRCs were

washed twice in cold phosphate buffered saline (PBS) and lysed with extraction buffer (20 mM NaPO4, 150 mM NaCl, 2 mM MgCl2, 0.1% Nonidet P-40, 10% glycerol, 10 mM sodium fluoride, 0.1 mM sodium orthovanadate, 10 mM sodium pyrophosphate, 100 μM phenylasine oxide, 10 nM okadaic acid, 1 mM dithiothreitol, 10 μg/ml leupeptin, 10 μg/ml aprotinin, 10 μg/ml pepstatin, 10 μg/ml tosyl-l-phenylalanine chloromethyl ketone, and 10 μg/ml *N*-tosyl-l-lysine chloromethyl ketone). After centrifugation for 30 min at 13000×*g*, supernatants were collected and protein concentration quantified. Equal amounts of protein were loaded to polyacrylamide gel for electrophoresis, and then transferred to polyvinylidene difluoride membranes (GE Healthcare). After being blocked with 5% milk dissolved in TBST (tris-buffered saline containing 1% tween 20) for 1 h, the blots were incubated with primary antibodies overnight at 4 °C. Afterwards, the blots were incubated in 2.5% milk with a horseradish peroxidase-conjugated secondary antibody for 1 h at room temperature and then processed for chemiluminescent detection using an ECL Advanced Western blotting kit (GE Healthcare). Protein abundance on Western blots was quantified by densitometry with the Quantity One program from Bio-Rad. Glyceraldehyde-3-phosphate dehydrogenase (GAPDH), β-actin and extracellular signal-regulated kinase 2 (ERK2) were purchased from Santa Cruz (Santa Cruz, CA). Anti-phosphoserine antibody was purchased from Abcam (Cambridge, MA). The following primary antibodies were purchased from Cell Signaling Technology (Danvers, MA): cleaved caspase 3, poly(ADP-ribose) polymerase (PARP), beclin 1, Sequestosome 1/P62 (p62), p70 S6 kinase (p70S6K), phospho-p70S6K (Thr-389), S6 Ribosomal Protein (S6), phospho-S6 (Ser-240), PRAS40, phospho-PRAS40 (Thr-264), Tuberin/TSC2, phospho-Tuberin/TSC2 (Thr-1462), Microtubule-associated protein light chain 3 (LC3), Autophagy-related 5 (Atg 5), and Atg12.

Construction and Utilization of Replication-deficient Adenoviruses. Adenovirus encoding GFP-LC3 was kindly provided by Dr. Tolkovsky. Adenoviruses expressing β-galactosidase (Adβgal), human beclin 1 (AdBCN1), the short hairpin RNA (shRNA) targeting rat Beclin 1 mRNA (AdshBCN1), and control shRNA (AdshCon) were created as previously

JPET Fast Forward. Published on December 30, 2011 as DOI: 10.1124/jpet.111.189589
This article has not been copyedited and formatted. The final version may differ from this version.

described (Kobayashi et al., 2010). To generate adenoviral vector expressing S6K1, an insert containing S6K1 cDNA sequence was amplified by PCR from GFP-tagged ORF clone of Mus musculus ribosomal protein S6 kinase (OriGene, MG208420) and integrated into the TA cloning vector (Invitrogen). The insert was then released from TA vector and sub-cloned into pShuttle-CMV vector via the BamHI-BglII (compatible ligation) and SalI restriction enzyme sites. Recombinant adenoviruses expressing S6K1 were then generated and amplified using the AdEasy Adenoviral Vector System (Stratagene). Unless otherwise indicated, a multiplicity of infection (MOI) of 20 plaque-forming units of each virus was used to infect cardiomyocytes. Two hours after incubation, infection medium was replaced by regular DMEM containing 1% bovine serum for an additional 24 h.

siRNA Gene Silencing. Pre-selected siRNAs targeting rat S6 kinase 1 mRNA (4390815) and a Silencer Negative Control siRNA #1 (AM4635) were obtained from Ambion (Austin, TX). The transfection was performed following the protocol provided by Ambion with minor modifications. 0.7×10^6 cardiomyocytes were used for transfection in each 6 mm dish. The culture media were replaced 24 h before transfection with fresh serum and antibiotic-free DMEM. Transfections were performed with 10 nM siRNA oligos, an optimized concentration to knock down S6K1. siRNA oligos in 200 µl Opti-MEM (Invitrogen) were mixed with Lipofectamine RNAiMAX (5 µl in 200 µl Opti-MEM), and incubated for 15 minutes. The mixture was then added dropwise to the culture dish with 2 ml media. The transfected cells were cultured for 12 h and fresh media were added. After another 36 h, the cells were treated with DOX and/or resveratrol for the indicated time, and then harvested. The drug effects and gene silencing efficiency were evaluated with Western blot analysis and the other assays as indicated in each experiment.

Cell Death Assay. Propidium iodide (PI, Roche Applied Science) was used to measure cardiomyocyte death. PI can enter dead cells through disrupted membranes to bind DNA that display as red dots under fluoresceence microscopy. A PI stock solution (0.5 µg/ml) was added

JPET Fast Forward. Published on December 30, 2011 as DOI: 10.1124/jpet.111.189589
This article has not been copyedited and formatted. The final version may differ from this version.

directly to the culture medium with 1:1000 dilutions. After 10 minutes, the cells were examined with a fluorescence microscope, and photographed under phase contrast or fluorescent condition. The PI-positive cells (stained red) were counted and expressed as a percentage against the total number of cells examined (200 to 250 counted under phase contrast).

Apoptosis Assays. Apoptosis analysis was determined by both DNA laddering assay and analysis of apoptotic proteins including the cleaved caspase 3 and PARP. DNA laddering assay was performed using a DNA laddering kit from Maxim Biotech, Inc. (San Francisco, CA). Briefly, the cells were harvested and genomic DNA were extracted and quantified. Equal amount of genomic DNA were ligated with specific adaptors for 14 hours and then subjected to PCR amplification. The PCR products were loaded to a 1.5% agrose gel, run for 40 minutes with a constant voltage of 250 volts/15cm, and then examined under UV light. Cleaved caspase 3 and PARP were determined by Western blot analysis as described above.

S6K1 kinase activity assay. S6K1 activity was measured by an immune-complex kinase assay using myelin basic protein (MBP) as the substrate. Briefly, cardiomyocytes were lysed and sonicated in lysis buffer composed of 40 mM Tris-HCl (pH 7.4), 137 mM NaCl, 25 mM sodium β-glycerophosphate, 2 mM sodium pyrophosphate, 2 mM EDTA, 1 mM sodium vanadate, 10% glycerol, 1% Triton X-100, leupeptin (5 μg/ml), aprotinin (5 μg/ml) and 1 mM PMSF. Homogenates were cleared by centrifugation for 5 min at 15,000 × g at 4 °C. Supernatants containing 100 μg of proteins were then incubated with anti-S6K1 antibodies (Cell Signaling, Danvers, MA) for 16 h followed by incubation with Protein A/G-agarose beads (Santa Cruz, CA) for 1 h. Beads were washed with lysis buffer 2 times and kinase reaction buffer (20 mM MOPS pH 7.2, 25 mM β-glycerophosphate, 5 mM EGTA, 1 mM sodium vanadate, and 1 mM DTT.) 2 times. An aliquot of precipitates was subjected to immunoblotting using anti-S6K1 antibody. The rest of the precipitates was then added with 10 μg dephosphorylated MBP (Upstate,) and 10 μl Mg/ATP Cocktail (500 μM ATP, 75mM MgCl2) in kinase reaction buffer. After incubation at 30°C for 30 minutes, the precipitates containing phosphorylated MBP were

subjected to Western blot analysis using anti-phosphoserine antibody. ERK2 antibodies and regular IgG were used as positive and negative controls, respectively.

Statistical Analysis. Data were presented as the mean ± SE. One-way or two-way analysis of variance (ANOVA) were used to analyze the differences between experimental groups followed by Tukey post-test using Prism software (GraphPad). Student's *t* tests for paired data were also used in some cases as indicated. *p* values < 0.05 were considered statistically significant.

RESULTS

Resveratrol protected against DOX-induced cardiomyocyte death. The effects of resveratrol on cardiomyocytes are strictly dose-dependent (Gurusamy et al., 2010). Therefore, we first determined if different doses of resveratrol would differentially impact the viability of neonatal rat ventricular cardiomyocytes (NRCs). NRCs were exposed to a series of doses of resveratrol for 24 h and the viability of NRCs was examined by PI staining that marks dead cells regardless of the cause of death, and the cleavage of caspase 3 or PARP that indicates apoptosis. When used at relatively low doses (<15 μM), resveratrol (RV) did not have any effect on the percentage of PI positive cells (Fig. 1A, *control 10.0±1.5 versus RV 10μM 10.7±2.1, p>0.05, n=4*). However, at higher doses (≥15 μM), resveratrol induced cardiomyocyte death as indicated by increased PI positive cells (Fig. 1A, *10μM 10.7±2.1 versus 15 μM 21.1±1.3, p<0.05, n=4*) and elevated cleavage of caspase 3 and PARP (Fig. 1B), suggesting that high dose resveratrol is toxic to cardiomyocytes. Since resveratrol has been reported to reduce DOX cardiotoxicity (Danz et al., 2009; Tatlidede et al., 2009), we then tested whether resveratrol at 10 μM could protect against DOX-induced cardiomyocyte death. As expected, pre-treatment of cells with resveratrol markedly diminished DOX-induced cardiomyocyte death as shown by PI positive cells (Fig. 1C, *control 10.2±0.5 versus DOX 43.7±4.2, p<0.01; DOX 43.7±4.2 versus DOX+RV 19.8±0.35, p<0.01, n=4*), DNA laddering (Fig. 1D), and cleaved

JPET Fast Forward. Published on December 30, 2011 as DOI: 10.1124/jpet.111.189589
This article has not been copyedited and formatted. The final version may differ from this version.

caspase 3 and PARP (Fig. 1E). Our results indicated that resveratrol is sufficient to attenuate DOX-induced cardiomyocyte death.

Resveratrol diminished DOX-induced autophagy in cardiomyocytes. DOX can induce autophagy in cardiomyocytes, which is a major mechanism of DOX cardiotoxicity (Lu et al., 2009; Kobayashi et al., 2010; Chen et al., 2011). Therefore, we tested if resveratrol could inhibit DOX-induced autophagy. When autophagy is induced, microtubule-associated protein light chain 3 (LC3) form I is converted to LC3-II and conjugated to the autophagosome membrane. LC3-II remains associated with autophagic vacuoles (AVs) until being degraded by lysosomal proteases (Kabeya et al., 2000). AV formation can be visualized by increased punctate structures (dots) of the GFP-LC3 fusion protein that is introduced into cells (Mizushima et al., 2010). Thus, autophagy can be measured by the amount of LC3-II protein or the number of GFP-LC3 dots formed. To differentiate whether the accumulation of LC3-II protein or GFP-LC3 dots is caused by an increased AV formation or a decreased degradation, it is necessary to measure the difference in LC3-II protein levels or GFP-LC3 dots in the absence and presence of a lysosomal inhibitor. This difference is referred to as autophagic flux that reflects the number of AVs that are delivered to and degraded in the lysosome (Mizushima and Yoshimori, 2007; Mizushima et al., 2010). To this end, we infected NRCs with an adenovirus encoding GFP-LC3. NRCs were pre-treated with resveratrol (10 μM) for 12 h and then exposed to DOX (1 μM) for another 18 hours. The lysosomal inhibitor bafilomycin A1 (BFA, 50 nM) was added 6h before the cells were examined for GFP-LC3 dots (AVs) under a confocal microscope. In line with previous reports (Lu et al., 2009; Kobayashi et al., 2010; Chen et al., 2011), DOX triggered the formation of numerous AVs as indicated by the GFP-LC3 dots, which was further increased by BFA treatment (Fig. 2A), suggesting that DOX accelerated autophagic flux in cardiomyocytes. However, the number of GFP-LC3 dots was dramatically reduced by resveratrol pre-treatment, demonstrating the ability of resveratrol to inhibit DOX-induced autophagic flux. We counted cells

JPET Fast Forward. Published on December 30, 2011 as DOI: 10.1124/jpet.111.189589
This article has not been copyedited and formatted. The final version may differ from this version.

with more than 25 GFP-LC3 dots, an arbitrary cut-off number that defines a cell as positive for increased AVs. Again, DOX increased the percentage of AV positive cells with and without BFA treatment, which was largely inhibited by resveratrol (right panel of Fig. 2A, *control 5.7±0.35 versus DOX 29.5±2.9, p<0.01; DOX 29.5±2.9 versus DOX+RV 9.2±0.8, p<0.01, n=3*).

Alternatively, the autophagic flux was quantified by the difference of endogenous LC3-II protein levels in the absence and presence of BFA. In this case, autophagic flux is indicated by the fold increase (the numbers above bars) of LC3II protein levels after BFA treatment. Similar to the results obtained with GFP-LC3 dots, autophagic flux was increased by DOX-treatment, which was prevented by resveratrol (Fig. 2B, *control 0.45±0.11 versus DOX 2.67±0.15, p<0.01; DOX 2.67±0.15 versus DOX+RV 0.64±0.09, p<0.01, n=3*). We also determined p62 protein levels to assess autophagic flux. p62/SQSTM1 is a polyubiquitin-binding protein, which is degraded by autophagy, and its protein levels are inversely related to autophagy activity (Komatsu et al., 2007; Mizushima and Yoshimori, 2007; Nakai et al., 2007). As shown in Fig. 2B (Western blot on the right), DOX decreased p62 levels, which was attenuated by resveratrol. Similarly, DOX increased the levels of autophagy related protein 5 (Atg5) and Atg5-Atg12 complex. However, resveratrol reversed this effect. Taken together, these results demonstrated that resveratrol is able to inhibit DOX-induced autophagy. Since low dose resveratrol was shown to induce autophagy in H9c2 cardiac myoblast cells (Gurusamy et al., 2010), we tested if this holds true in primary cardiomyocyte culture. We found that resveratrol at lower doses (0.1~1 μM) did not affect autophagic flux (data not shown).

The ability of resveratrol to antagonize DOX-induced cardiomyocyte death is mediated through autophagy inhibition. Induction of autophagy could be an adaptive response to protect cell from environmental stresses. However, enhanced autophagy can also trigger cell death under certain conditions (Matsui et al., 2007; Kang and Avery, 2008). Indeed, DOX induced-autophagy contributes to the cardiomyocyte death, which is a major mechanism of DOX cardiotoxicity (Lu et al., 2009; Kobayashi et al., 2010; Chen et al., 2011). Given the

ability of resveratrol to concurrently suppress DOX-induced autophagy and cardiomyocyte death, it is possible that the protective effects of resveratrol against DOX toxicity are mediated through autophagy inhibition. To test this possibility, we infected cardiomyocytes with adenoviruses encoding either autophagy-related protein beclin1 or β-gal, and 36 hours later treated cells with DOX in the absence or presence of resveratrol. Overexpression of beclin 1 accelerated autophagic flux as evidenced by increased LC3-II levels with or without BFA treatment (Fig. 3A, *Adβgal 0.62±0.07 versus AdBCN1 1.05±0.13, p<0.01, n=3*), which enhanced DOX-induced cardiomyocyte death as shown by PI staining (Fig. 3B&C, *Adβgal+DOX 44±4.4 versus AdBCN1+DOX 73±9.3, p<0.01, n=3*), DNA laddering (Fig. 3D) and the cleavage of caspase 3 and PARP (Fig. 3E). Resveratrol blocked DOX-induced cardiomyocyte death in Adβgal-infected cells, but this ability was abrogated in AdBCN1-infected cells (Fig. 3B&C, PI positive cells, *AdBCN1+DOX 73±9.3 versus AdBCN1+DOX+RV 69±8.1, p>0.05, n=3*). These results demonstrate that up-regulation of autophagy by beclin 1 over-expression enhanced DOX-induced cardiotoxicity and abolished the protective effects of resveratrol, suggesting that autophagy suppression is critical for resveratrol to antagonize DOX-induced cardiomyocyte death.

To further corroborate the role of autophagy inhibition in resveratrol-mediated cytoprotection, we determined the cardioprotective effects of resveratrol in the presence of autophagy inhibitor 3-methyladenine (3-MA). Cardiomyocytes were treated with DOX, resveratrol and 3-MA (2.5mM), either alone or in combination for 18 hours. PI staining showed that DOX-induced cell death was attenuated by 3-MA, but it was not further reduced by resveratrol (Fig. 4A, *DOX 43.4±6.01 versus DOX+3-MA 24.9±3.4 p<0.01; DOX+3-MA 24.9±3.4 versus DOX+3-MA+RV, 28.1±2.6, p>0.05, n=4*). Similarly, DOX-induced DNA laddering was mitigated by either 3-MA or resveratrol alone, but both drugs together did not produce additive effects (Fig. 4B). To rule out the potential non-specific effects of 3-MA, we down-regulated autophagy in cardiomyocytes with an adenovirus encoding a short hairpin RNA against beclin 1

JPET Fast Forward. Published on December 30, 2011 as DOI: 10.1124/jpet.111.189589
This article has not been copyedited and formatted. The final version may differ from this version.

(shBCN1). A scrambled shRNA (shCON) was used as control. Autophagic flux was significantly reduced following beclin 1 knockdown as indicated by the decreased LC3-II protein levels (Fig. 4C, *shCON 0.68±0.4 versus shBCN1 0.38 ±0.3, p<0.05, n=3*). Similar to 3-MA, beclin 1 knockdown attenuated DOX-induced cardiomyocyte death as shown by PI staining (Fig. 4D, *DOX 45.7±5.11 versus DOX+shBCN1 26.4±2.4, p<0.01, n=4*), which was not further reduced by resveratrol (*DOX+shBCN1 26.4±2.4 versus DOX+shBCN1+RV, 22.4±2.3, p>0.05, n=4*). Also, resveratrol did not further enhance the effects of beclin 1 knockdown on DOX-induced DNA laddering (Fig 4E) and cleavage of caspase 3 and PARP (Fig. 4F). Together, these results indicate that down-regulation of autophagy by either 3-MA or beclin 1 knockdown alleviated DOX induced cardiotoxicity, but resveratrol failed to exert an additive effect. Thus**,** our data from studies with either up- or down-regulation of autophagy strongly suggest that the protective effects of resveratrol against DOX cardiotoxicity are likely mediated through its ability to inhibit autophagy.

DOX activated p70 S6 Kinase 1 (S6K1), which was prevented by resveratrol. To explore the underlying molecular mechanisms that mediate the ability of resveratrol to inhibit DOX-triggered autophagy in cardiomyocytes, we examined several signaling pathways known to either positively or negatively regulate autophagy. The intracellular energy sensor AMP-activated protein kinase (AMPK) is a positive regulator of autophagy. DOX and resveratrol, either alone or in combination, did not have appreciable effects on AMPK activity as indicated by Western blot analysis of phosphorylated AMPKα, AMPKβ and its downstream target Acetyl-CoA Carboxylase (data not shown), suggesting that AMPK might not be involved in autophagy induction by DOX or its subsequent inhibition by resveratrol. In addition, we found that DOX robustly induced AKT signaling, as shown by the increased phosphorylation of ATK at Thr-308 and Ser-473 and its downstream effecter GSK-3β at Ser-9. This DOX effect was completely reversed by resveratrol (data not shown). However, since AKT is a negative regulator of autophagy, the above specific changes in AKT signaling are unlikely responsible for autophagy

induction by DOX and its inhibition by resveratrol. We then examined the effects of DOX and/or resveratrol on the mammalian target of rapamycin (mTOR). DOX enhanced mTOR signaling as shown by the increased phosphorylation of mTOR downstream targets S6K and S6 (Fig. 5A). Given that mTOR is a kinase that in general negatively regulates autophagy, this result did not seem to support a role for mTOR in DOX-induced autophagy. Moreover, resveratrol largely inhibited mTOR signaling either in the absence or presence of DOX, as indicated by the reduced phosphorylation of TSC2, PRAS40, S6K, and S6 (Fig. 5A). Apparently, the general inhibitory effects of resveratrol on mTOR signaling did not appear to be compatible with its ability to antagonize DOX-induced autophagy. Intriguingly, however, S6K1 has been shown to positively regulate autophagy independent of mTOR signaling in some context (Scott et al., 2004) and has been proposed to mediate the inhibitory effect of resveratrol on autophagy in human NIH3T3 and HEK293 cells (Armour et al., 2009). In this respect, DOX treatment led to a 6.77-fold increase in the phosphorylation of S6K1 on Thr-389, which was drastically reduced by resveratrol (Fig. 5A, *DOX 6.77±1.36 versus DOX+RV 2.69±0.69, p<0.05, n=4*). We further measured the kinase activity of S6K1 under these conditions by an immuno-complex kinase assay using MBP as the substrate. As shown in Fig. 5B, resveratrol did not affect S6K1 activity at baseline, but it inhibited DOX-induced S6K1 activation, consistent with the phosphorylation levels of S6K1 and its downstream target S6. Thus, these results raise the possibility that DOX may induce autophagy in cardiomyocytes through S6K1 activation, and resveratrol may prevent autophagy induction by inhibiting S6K1 signaling.

S6K1 knockdown attenuated DOX induced autophagy and cardiomyocyte death, but resveratrol failed to exert an additive effect. To characterize the role of S6K1 in DOX-induced autophagy and cardiomyocyte death, we knocked down S6K1 expression with siRNA. Cardiomyocytes were transfected with a control siRNA (siCON) or a siRNA against S6K1 (siS6K1), and then treated with DOX at 36 h after transfection. Western blot analysis showed that siS6K dramatically reduced S6K1 protein levels and its phosphorylation on Thr-389 (Fig.

JPET Fast Forward. Published on December 30, 2011 as DOI: 10.1124/jpet.111.189589
This article has not been copyedited and formatted. The final version may differ from this version.

6A), indicating the effectiveness of the siRNA-mediated S6K1 gene silencing. We then performed autophagic flux assays as described earlier. DOX accelerated autophagic flux, which was blocked by S6K1 knockdown, as quantified by the difference of endogenous LC3-II protein levels in the absence and presence of BFA (Fig. 6B & 6D, *DOX 2.40±0.21 versus DOX+siS6K1 0.58±0.08, p<0.01, n=4)*. Also, the autophagic flux was determined with GFP-LC3 reporter. DOX induced the formation of numerous AVs indicated by the GFP-LC3 dots, while S6K1 knockdown markedly attenuated AV formation (Fig. 6C). Quantitatively, DOX increased the percentage of AV positive cells with or without BFA intervention, which was largely inhibited by S6K1 knockdown (Fig. 6E, *DOX 30.7±5.2 versus DOX+siS6K1 6.1±3.1, p<0.01, n=4*). These results confirmed the ability of S6K1 knockdown to block DOX-induced autophagic flux, suggesting an essential role for S6K in autophagy induction. Of note, following S6K1 knockdown, DOX-induced autophagic flux was not further reduced by addition of resveratrol as evidenced by LC3-II levels (Fig. 6D, *DOX+siS6K1 0.58±0.08 versus DOX+siS6K1+RV 0.66±0.13 p>0.05, n=4)* and AV positive cells (Fig. 6E, *DOX+siS6K1 6.1±3.1 versus DOX+siS6K1+RV 8.3±2.2, p>0.05, n=4*). These data support the notion that resveratrol may inhibit DOX-induced autophagy through its suppressing effect on S6K1.

We next examined cell death following S6K1 knockdown. DOX-induced cell death was significantly inhibited by S6K1 knockdown, and the addition of resveratrol failed to exert an additive effect, as indicated by PI positive cells (Fig. 7A&B, *DOX 45.0±4.21 versus DOX+siS6K 31±3.88, p<0.05; DOX+siS6K 31±3.8 versus DOX+siS6K+RV 32±2.06 p>0.05 n=3*), DNA laddering (Fig. 7C) as well as the cleavage of caspase 3 and PARP (Fig. 7D). Again, these results raise the possibility that the cardioprotective effects of resveratrol may be mediated through S6K1 inhibition.

Overexpression of S6K1 did not enhance DOX-induced autophagy and cardiomyocyte death, but it abolished the protective effects of resveratrol. The results from the above loss-of-function experiments demonstrate an essential role for S6K1 in DOX-

induced autophagy and cardiomyocyte death. Resveratrol per se is sufficient to reduce DOX cardiotoxicity, but it cannot further enhance the protective effect of S6K1 knockdown, suggesting S6K1 inhibition as a major mechanism that mediates the ability of resveratrol to antagonize DOX cardiotoxicity. If this is true, overexpression of S6K1 should attenuate or abolish the protective effects of resveratrol. To test this possibility, we infected cardiomyocytes with adenoviruses encoding either β-gal or S6K1. As shown in Fig. 8A, adenovirus-mediated gene transfer increased the protein levels of S6K in a MOI (multiplicity of infection) dependent manner, leading to elevated phosphorylation levels of S6, a downstream target of S6K1 (Fig. 8A). We then determined if S6K1 overexpression could affect autophagy in cardiomyocytes with or without DOX treatment. To our surprise, increasing S6K1 expression did not induce autophagy, nor did it further accelerate DOX-triggered autophagic flux, as shown by the LC3-II protein levels (Fig. 8B&D, *DOX 2.1±0.31 versus DOX+AdS6K1 2.2±0.28, p>0.05 n=3*) and the percentages of AVs positive cells before and after BFA treatment (Fig. 8C&E). Strikingly, when S6K1 was overexpressed, resveratrol can no longer inhibit DOX-induced autophagy as indicated by either LC3-II (Fig. 8B&D, *DOX+AdS6K1 2.2±0.28 versus DOX+AdS6K1+RV, 2.0±0.30 p>0.05 n=3*) or AV positive cells (Fig. 8C&E, *DOX+AdS6K1 38±7.28 versus DOX+AdS6K1+RV, 32±8.50 p>0.05 n=3*). These data strongly suggest that S6K1 inhibition is important for resveratrol to suppress autophagic activity in cardiomyocytes treated with DOX.

Also, we measured cardiomyocyte death under this condition. Although S6K1 overexpression did not affect DOX-induced cell death, it markedly compromised the ability of resveratrol to reduce DOX cytotoxicity, as shown by PI staining (Fig. 9A&B *DOX 44.0±3.21 versus DOX+AdS6K1 46±3.88, p>0.05; DOX+AdS6K1 46±3.88 versus DOX+AdS6K1+RV 42±4.08, p>0.05, n=4*), the cleavage of caspase 3 and PARP (Fig. 9C) as well as DNA laddering (Fig. 9D). These observations suggest the inhibition of S6K1 as an important underlying mechanism that mediates the protective effects of resveratrol against DOX cardiotoxicity.

DISCUSSION

DOX-induced cardiotoxicity is the major obstacle that limits its therapeutic usage in cancer chemotherapy (Minotti et al., 2004). Dexrazoxane is the only drug approved by the FDA to reduce DOX cardiotoxicity, yet its combined use with DOX has been limited, due to fears of its negative effect on the anti-tumor efficacy of DOX (Tebbi et al., 2007). However, resveratrol has been shown to enhance the anti-cancer activity of DOX and at the same time to exert cardioprotective effects (Aggarwal et al., 2004; Rezk et al., 2006), raising the possibility that the combined use of resveratrol and DOX may be a viable chemotherapeutic modality that will find increased use in DOX antitumor therapy in the near future. The mechanisms by which resveratrol could deliver cardiac beneficial effects in the setting of DOX chemotherapy remain poorly understood. In the present study, we demonstrated that DOX-induced cardiomyocyte death was dramatically reduced by resveratrol, and this protective effect was largely dependent on the ability of resveratrol to suppress autophagy. Our data also indicates that p70 S6 kinase (S6K1) is a critical molecular mediator of DOX-induced autophagy and cardiomyocyte death, and that inhibiting S6K1 is important for resveratrol to prevent autophagy induction and reduce DOX cardiotoxicity.

Resveratrol-conferred protection against DOX cardiotoxicity is associated with increased superoxide dismutase activity and reduced production of reactive oxygen species (Tatlidede et al., 2009), suggesting that the antioxidant properties of resveratrol may play a role in its cardioprotective effects. However, antioxidant therapies have failed to produce satisfactory results in clinical trials (Gianni et al., 2008), casting doubt on the notion that the inhibition of oxidative stress is the only mechanism responsible for the cardioprotective effects of resveratrol. In this respect, we found that the ability of resveratrol to attenuate DOX-induced cardiomyocyte death is dependent on autophagy suppression, providing another explanation for the protective effects of resveratrol. Since oxidative stress can induce autophagy triggering autophagic cancer cell death (Chen et al., 2008), it is possible that resveratrol-elicited autophagy inhibition may

result, at least in part, from its ability to antagonize DOX-induced oxidative stress. However, given the failure of antioxidant therapies in cancer patients that receive DOX, it is more likely that autophagy suppression is an independent mechanism by which resveratrol attenuates DOX cardiotoxicity.

Autophagy is a catabolic process involving the degradation of a cell's own components through the lysosomal machinery, which can be either protective or detrimental depending on the specific cellular context. DOX-induced autophagy in cardiomyocytes is detrimental since inhibiting autophagy with chemical or genetic approach dramatically attenuates DOX-induced cardiomyocyte death as shown previously (Lu et al., 2009; Kobayashi et al., 2010; Chen et al., 2011). Thus, a potential therapeutic strategy to reducing DOX cardiotoxicity is to suppress DOX-induced autophagy. Consistently, the transcription factor GATA4 and the caloric restriction mimetic 2-deoxyglucose are able to inhibit DOX-induced autophagy thereby reducing cardiomyocyte death (Kobayashi et al., 2010; Chen et al., 2011). To reinforce this concept, resveratrol is also capable of antagonizing DOX cardiotoxicity through autophagy inhibition (Figs. 2, 3&4). Similarly, resveratrol attenuates starvation-induced autophagy in multiple non-cardiac mammalian cell lines although its effect on cell viability is unknown (Armour et al., 2009).

However, resveratrol has been shown to enhance hypoxia-reoxygenation-induced autophagy in H9c2 cardiac myoblast cells at low doses (0.1 and 1 μM), which correlates with improved cell survival (Gurusamy et al., 2010). The same study has also demonstrated that high dose resveratrol (100 μM) inhibits autophagy leading to increased cell death. Moreover, resveratrol can induce autophagy in multiple ovarian carcinoma cell lines, which appears to cause cell death (Opipari et al., 2004). Apparently, the specific effects of resveratrol on autophagy and cell fate are dependent on multiple factors including drug dose, cell type as well as the nature, degree and duration of the stress placed on the cell.

JPET Fast Forward. Published on December 30, 2011 as DOI: 10.1124/jpet.111.189589
This article has not been copyedited and formatted. The final version may differ from this version.

Intriguingly, our study not only demonstrated that resveratrol attenuated DOX cardiotoxicity by suppressing autophagy, but also suggested that the ability of resveratrol to prevent DOX-induced autophagy is likely mediated through its inhibitory effect on S6K1. The evidence is three-fold: first, the phosphorylation of S6K1 is significantly elevated in response to DOX treatment but largely prevented by addition of resveratrol; second, S6K1 knockdown attenuated DOX-induced autophagy, which was not further reduced by resveratrol; and finally, S6K1 overexpression abolished the effect of resveratrol on DOX-induced autophagy, suggesting that suppressing S6K1 may be important for resveratrol to inhibit autophagy. Nevertheless, we cannot completely rule out other possibilities that may explain the relationship between S6K and resveratrol. For instance, resveratrol may not protect the cells through directly inhibiting S6K. Rather, it could act on a downstream effecter to provide cardioprotection. Also, the ability of S6K overexpression to antagonize resveratrol action could be mediated by the opposing effects of S6K and resveratrol on an unidentified common target. In addition, overexpression of S6K could modify the cellular response to DOX such that DOX induces autophagy and cell death through a different pathway that is insensitive to resveratrol. However, these speculations can only be confirmed by further experimentations.

At first sight, the observation that S6K1 positively regulates autophagy upon DOX exposure seems contradictory to the fact that S6K is a downstream effecter of mTOR, a well established negative regulator of autophagy. Indeed, previous studies demonstrated that inhibition of S6K kinase can induce autophagy (Lee et al., 2007), while activation of ribosomal protein S6 can suppress autophagy (Blommaart et al., 1995). However, accumulating evidence has suggested that S6K can contribute to autophagy induction under many other conditions. For example, S6K1 can positively regulate 6-thioguanine-induced autophagy (Zeng and Kinsella, 2008). In *Drosophila* fat body, S6K promotes rather than suppresses autophagy in response to starvation (Scott et al., 2004). Except for the gain-of-function studies, knockdown of both S6K1 and S6K2 genes decreased starvation-dependent GFP-LC3 conversion in 293A cells (Chan et

al., 2007). Similarly, inhibition of S6K1 by either shRNA or dominant-negative S6K1 mutant suppresses autophagy in HEK293 cells (Armour et al., 2009). Collectively, these results demonstrate that whether S6K1 positively or negatively regulates autophagy depends on specific cellular contexts such as cell type, culture condition and the nature of the treatment. Nevertheless, the underlying molecular mechanisms that confer the pro- or anti-autophagy property of S6K remain poorly understood. One possible explanation for the pro-autophagy function of S6K is that S6K1 negatively regulates insulin signaling (Shah et al., 2004). The latter normally inhibits autophagy.

Our data also demonstrated that S6K1 knocking down markedly attenuated DOX-induced cardiomyocyte death, suggesting that S6K1 activation is required for DOX to induce cardiotoxicity. Although S6K1 overexpression is not sufficient to enhance DOX cardiotoxicity, it abolishes the protective effect of resveratrol. Apparently, our observation that S6K1 mediates DOX cardiotoxicity challenges a long standing view that S6K1 acts downstream of mTOR to promote cell growth and survival. One possibility is that S6K1 may control either pro-survival or pro-death signaling in response to different environmental stimuli. When nutrients are abundant to favor cell growth, S6K1 is activated by mTOR to exert pro-survival effects. On the other hand, when dealing with excessive stress, S6K1 can activate cell death pathway which is likely independent of mTOR signaling. Notably, in support of a pro-death role of S6K1, several studies have demonstrated that down-regulation of S6K1 is protective. For instance, S6K1 deficiency is able to protect against hepatocyte apoptosis (Gonzalez-Rodriguez et al., 2009). In yeast, deletion of Sch9, the homolog of mammalian S6K/Akt, protects against age-dependent defects and extends chronological lifespan (Wei et al., 2008). In *Drosophila*, expression of a dominant negative S6K1 results in resistance to oxidative stress (Patel and Tamanoi, 2006). Importantly, deletion of S6K1 is sufficient to extend mouse lifespan (Selman et al., 2009), underscoring the beneficial nature of down-regulating S6K1 signaling. Therefore, resveratrol-conferred protection

against DOX cardiotoxicity could be attributed, at least in part, to its ability to inhibit S6K1 as well as autophagy.

In summary, our study demonstrates that resveratrol is able to attenuate DOX-induced cardiomyocyte death, which is largely dependent on its ability to inhibit autophagy. Our results have also suggested that the inhibition of S6K1 is a critical event that likely mediates the ability of resveratrol to suppress DOX-induced autophagy and cytotoxic effects. Therefore, therapeutic strategies that aim to reduce S6K1 signaling and autophagic activity will presumably be able to ameliorate DOX cardiotoxicity, leading to improved clinical use of DOX in cancer chemotherapy.

ACKNOWLEDGMENTS:

The authors would like to thank Andy Cypher in Cell Culture Core Facility at the Sanford Research/USD for providing cultured cardiomyocytes, and Tricia Krueger and Yuan Huang in Virus Core Facility for preparing several adenoviruses used in this work. We also thank Imaging Core Facility for assistance in confocal microscopy. These core facilities are supported by NIH grant 2P20RR017662-06A1. We are grateful to Dr. Aviva Tolkovsky at the University of Cambridge for providing the adenovirus expressing GFP-LC3.

AUTHORSHIP CONTRIBUTIONS:

Participated in research design: Liang, Xu.

Conducted experiments: Xu, Chen, and Kobayashi.

Contributed new regents or analytic tools: Xu, Kobayashi, Derek.

Performed data analysis: Xu, Chen, Kobayashi

Wrote or contributed to the writing of the manuscript: Liang, Xu

REFERENCES

Aggarwal BB, Bhardwaj A, Aggarwal RS, Seeram NP, Shishodia S and Takada Y (2004) Role of resveratrol in prevention and therapy of cancer: preclinical and clinical studies. *Anticancer Res* **24**:2783-2840.

Akazawa H, Komazaki S, Shimomura H, Terasaki F, Zou Y, Takano H, Nagai T and Komuro I (2004) Diphtheria toxin-induced autophagic cardiomyocyte death plays a pathogenic role in mouse model of heart failure. *J Biol Chem* **279**:41095-41103.

Armour SM, Baur JA, Hsieh SN, Land-Bracha A, Thomas SM and Sinclair DA (2009) Inhibition of mammalian S6 kinase by resveratrol suppresses autophagy. *Aging (Albany NY)* **1**:515-528.

Baur JA and Sinclair DA (2006) Therapeutic potential of resveratrol: the in vivo evidence. *Nat Rev Drug Discov* **5**:493-506.

Blommaart EF, Luiken JJ, Blommaart PJ, van Woerkom GM and Meijer AJ (1995) Phosphorylation of ribosomal protein S6 is inhibitory for autophagy in isolated rat hepatocytes. *J Biol Chem* **270**:2320-2326.

Chan EY, Kir S and Tooze SA (2007) siRNA screening of the kinome identifies ULK1 as a multidomain modulator of autophagy. *J Biol Chem* **282**:25464-25474.

Chen K, Xu X, Kobayashi S, Timm D, Jepperson T and Liang Q (2011) Caloric Restriction Mimetic 2-Deoxyglucose Antagonizes Doxorubicin-induced Cardiomyocyte Death by Multiple Mechanisms. *J Biol Chem* **286**:21993-22006.

Chen Y, McMillan-Ward E, Kong J, Israels SJ and Gibson SB (2008) Oxidative stress induces autophagic cell death independent of apoptosis in transformed and cancer cells. *Cell Death Differ* **15**:171-182.

Danz ED, Skramsted J, Henry N, Bennett JA and Keller RS (2009) Resveratrol prevents doxorubicin cardiotoxicity through mitochondrial stabilization and the Sirt1 pathway. *Free Radic Biol Med* **46**:1589-1597.

Gianni L, Herman EH, Lipshultz SE, Minotti G, Sarvazyan N and Sawyer DB (2008) Anthracycline cardiotoxicity: from bench to bedside. *J Clin Oncol* **26**:3777-3784.

Gonzalez-Rodriguez A, Alba J, Zimmerman V, Kozma SC and Valverde AM (2009) S6K1 deficiency protects against apoptosis in hepatocytes. *Hepatology* **50**:216-229.

Gurusamy N, Lekli I, Mukherjee S, Ray D, Ahsan MK, Gherghiceanu M, Popescu LM and Das DK (2010) Cardioprotection by resveratrol: a novel mechanism via autophagy involving the mTORC2 pathway. *Cardiovasc Res* **86**:103-112.

Kabeya Y, Mizushima N, Ueno T, Yamamoto A, Kirisako T, Noda T, Kominami E, Ohsumi Y and Yoshimori T (2000) LC3, a mammalian homologue of yeast Apg8p, is localized in autophagosome membranes after processing. *EMBO J* **19**:5720-5728.

Kang C and Avery L (2008) To be or not to be, the level of autophagy is the question: dual roles of autophagy in the survival response to starvation. *Autophagy* **4**:82-84.

Kobayashi S, Mao K, Zheng H, Wang X, Patterson C, O'Connell TD and Liang Q (2007) Diminished GATA4 protein levels contribute to hyperglycemia-induced cardiomyocyte injury. *J Biol Chem* **282**:21945-21952.

Kobayashi S, Volden P, Timm D, Mao K, Xu X and Liang Q (2010) Transcription factor GATA4 inhibits doxorubicin-induced autophagy and cardiomyocyte death. *J Biol Chem* **285**:793-804.

Komatsu M, Waguri S, Koike M, Sou YS, Ueno T, Hara T, Mizushima N, Iwata J, Ezaki J, Murata S, Hamazaki J, Nishito Y, Iemura S, Natsume T, Yanagawa T, Uwayama J, Warabi E, Yoshida H, Ishii T, Kobayashi A, Yamamoto M, Yue Z, Uchiyama Y, Kominami E and Tanaka K (2007) Homeostatic

levels of p62 control cytoplasmic inclusion body formation in autophagy-deficient mice. *Cell* **131**:1149-1163.

Kuma A, Hatano M, Matsui M, Yamamoto A, Nakaya H, Yoshimori T, Ohsumi Y, Tokuhisa T and Mizushima N (2004) The role of autophagy during the early neonatal starvation period. *Nature* **432**:1032-1036.

Lee SB, Kim S, Lee J, Park J, Lee G, Kim Y, Kim JM and Chung J (2007) ATG1, an autophagy regulator, inhibits cell growth by negatively regulating S6 kinase. *EMBO Rep* **8**:360-365.

Lu L, Wu W, Yan J, Li X, Yu H and Yu X (2009) Adriamycin-induced autophagic cardiomyocyte death plays a pathogenic role in a rat model of heart failure. *Int J Cardiol* **134**:82-90.

Matsui Y, Takagi H, Qu X, Abdellatif M, Sakoda H, Asano T, Levine B and Sadoshima J (2007) Distinct roles of autophagy in the heart during ischemia and reperfusion: roles of AMP-activated protein kinase and Beclin 1 in mediating autophagy. *Circ Res* **100**:914-922.

Minotti G, Menna P, Salvatorelli E, Cairo G and Gianni L (2004) Anthracyclines: molecular advances and pharmacologic developments in antitumor activity and cardiotoxicity. *Pharmacol Rev* **56**:185-229.

Mizushima N and Yoshimori T (2007) How to interpret LC3 immunoblotting. *Autophagy* **3**:542-545.

Mizushima N, Yoshimori T and Levine B (2010) Methods in mammalian autophagy research. *Cell* **140**:313-326.

Nakai A, Yamaguchi O, Takeda T, Higuchi Y, Hikoso S, Taniike M, Omiya S, Mizote I, Matsumura Y, Asahi M, Nishida K, Hori M, Mizushima N and Otsu K (2007) The role of autophagy in cardiomyocytes in the basal state and in response to hemodynamic stress. *Nat Med* **13**:619-624.

Opipari AW, Jr., Tan L, Boitano AE, Sorenson DR, Aurora A and Liu JR (2004) Resveratrol-induced autophagocytosis in ovarian cancer cells. *Cancer Res* **64**:696-703.

Patel PH and Tamanoi F (2006) Increased Rheb-TOR signaling enhances sensitivity of the whole organism to oxidative stress. *J Cell Sci* **119**:4285-4292.

Rezk YA, Balulad SS, Keller RS and Bennett JA (2006) Use of resveratrol to improve the effectiveness of cisplatin and doxorubicin: study in human gynecologic cancer cell lines and in rodent heart. *Am J Obstet Gynecol* **194**:e23-26.

Scott RC, Schuldiner O and Neufeld TP (2004) Role and regulation of starvation-induced autophagy in the Drosophila fat body. *Dev Cell* **7**:167-178.

Selman C, Tullet JM, Wieser D, Irvine E, Lingard SJ, Choudhury AI, Claret M, Al-Qassab H, Carmignac D, Ramadani F, Woods A, Robinson IC, Schuster E, Batterham RL, Kozma SC, Thomas G, Carling D, Okkenhaug K, Thornton JM, Partridge L, Gems D and Withers DJ (2009) Ribosomal protein S6 kinase 1 signaling regulates mammalian life span. *Science* **326**:140-144.

Shah OJ, Wang Z and Hunter T (2004) Inappropriate activation of the TSC/Rheb/mTOR/S6K cassette induces IRS1/2 depletion, insulin resistance, and cell survival deficiencies. *Curr Biol* **14**:1650-1656.

Taneike M, Yamaguchi O, Nakai A, Hikoso S, Takeda T, Mizote I, Oka T, Tamai T, Oyabu J, Murakawa T, Nishida K, Shimizu T, Hori M, Komuro I, Shirasawa T, Mizushima N and Otsu K (2011) Inhibition of autophagy in the heart induces age-related cardiomyopathy. *Autophagy* **6**.

Tatlidede E, Sehirli O, Velioglu-Ogunc A, Cetinel S, Yegen BC, Yarat A, Suleymanoglu S and Sener G (2009) Resveratrol treatment protects against doxorubicin-induced cardiotoxicity by alleviating oxidative damage. *Free Radic Res* **43**:195-205.

Tebbi CK, London WB, Friedman D, Villaluna D, De Alarcon PA, Constine LS, Mendenhall NP, Sposto R, Chauvenet A and Schwartz CL (2007) Dexrazoxane-associated risk for acute myeloid leukemia/myelodysplastic syndrome and other secondary malignancies in pediatric Hodgkin's disease. *J Clin Oncol* **25**:493-500.

Wei M, Fabrizio P, Hu J, Ge H, Cheng C, Li L and Longo VD (2008) Life span extension by calorie restriction depends on Rim15 and transcription factors downstream of Ras/PKA, Tor, and Sch9. *PLoS Genet* **4**:e13.

Wood JG, Rogina B, Lavu S, Howitz K, Helfand SL, Tatar M and Sinclair D (2004) Sirtuin activators mimic caloric restriction and delay ageing in metazoans. *Nature* **430**:686-689.

Yen HC, Oberley TD, Vichitbandha S, Ho YS and St Clair DK (1996) The protective role of manganese superoxide dismutase against adriamycin-induced acute cardiac toxicity in transgenic mice. *J Clin Invest* **98**:1253-1260.

Zeng X and Kinsella TJ (2008) Mammalian target of rapamycin and S6 kinase 1 positively regulate 6-thioguanine-induced autophagy. *Cancer Res* **68**:2384-2390.

FOOTNOTES:

This work was supported by National Institutes of Health National Center for Research Resources [2P20RR017662-06A1]; Juvenile Diabetes Research Foundation Research Grant [1-2007-741]; and a Career Development Grant from the American Diabetes Association [1-09-CD-09].

Reprint request: Qiangrong Liang, Cardiovascular Health Research Center, Sanford Research/USD, 2301 East 60th St. Sioux Falls, SD 57104. E-mail: Qiangrong.Liang@sanfordhealth.org

LEGENDS FOR FIGURES:

Figure 1. **Resveratrol protected against DOX-induced cardiomyocytes death.** Dose response study was performed in A and B. Neonatal rat cardiomyocytes (NRCs) were cultured in DMEM with 2% bovine serum and treated with different doses of resveratrol (RV, 1-20μM) for 24 h. Cell death was determined by PI staining (A) and Western blot analysis of cleaved caspase3 (c-Casp3) and cleaved PARP (c-PARP) (B). c-Casp3 and c-PARP were sequentially normalized to GAPDH and the value at 0 μM RV. Data were expressed as mean ± SE and analyzed by one-way ANOVA (n=4). *p<0.05 and **p<0.01 versus 0-10 μM, # p<0.05 versus 15 μM. Ten μM of RV was selected for further study. NRCs were pre-treated with RV or vehicle for 12 h, and then exposed to either DOX (1 μM) or saline. Cardiomyocyte death was determined by PI staining (C), DNA laddering (D) and cleavage of caspase 3 and PARP (E). Data were expressed as mean ± SE and analyzed by one-way ANOVA (n=4). The scale bar in C is 1 mm. **p<0.01 versus control, # p<0.05 versus DOX.

Figure 2. **Resveratrol attenuated DOX-induced autophagy in cardiomyocytes.** NRCs were infected with a GFP-LC3 encoding adenovirus, and treated with resveratrol (RV, 10 μM) and DOX alone or together in the presence or absence of the lysosome inhibitor bafilomycin A1 (BFA). DOX increased the number of autophagic vacuoles (AVs) as shown by GFP-LC3 dots, which was prevented by RV (left panel of A). Autophagic flux was calculated as the percentage increase (the numbers above bars) of AV positive cells (right panel of A) or the fold increase of endogenous LC3II protein levels with and without BFA (upper left panel of B: Western blots; lower left panel of B: bar graph). P62 and autophagy related genes were also analyzed (upper right panel of B: Western blots; lower middle and right panels of B: bar graphs). Data were expressed as mean ± SE and analyzed by two-way ANOVA followed by paired student's *t* test (n=3). The *scale bar* in A is 50μm. **p<0.01, versus control, #p<0.05 versus DOX.

Figure 3. Up-regulation of autophagy by beclin 1 overexpression impaired the ability of resveratrol to antagonize DOX-induced cardiomyocyte death. NRCs were infected with Adβgal or AdBCN1 for 24 h. Autophagic flux was examined by Western blot analysis of LC3-II in the presence or absence of BFA (A). Cardiomyocytes were further treated with DOX (1 μM) alone or plus resveratrol (RV, 10μM), and cell death was determined by PI staining (B and C), DNA laddering (D) and cleavage of caspase 3 and PARP (E). Data were expressed as mean ± SE and analyzed by two-way ANOVA followed by paired student's *t* test (n=3-4). The *scale bar* in B is 500μm. *p<0.05,** p<0.01.

Figure 4. **Down-regulation of autophagy by 3-MA or beclin 1 knockdown alleviated DOX-induced cardiomyocyte death and resveratrol failed to exert an additive effect.** NRCs were treated with DOX, resveratrol and 3-MA (2.5mM), either alone or in combination for 18 h, and cell death was determined by PI staining (A) and DNA laddering (B). Alternatively, NRCs were infected with adenoviruses encoding either a control small hairpin RNA (shCON) or a shRNA against beclin1 (shBCN1) for 36 hours. shBCN1-mediated down-regulation of autophagy was confirmed by the inhibited autophagic flux as measured by the LC3-II protein levels in the presence or absence of BFA (C). Cardiomyocytes were then treated with vehicle, DOX (1 μM) or DOX plus RV (10μM), and cell death was determined by PI staining (D), DNA laddering (E), cleaved caspase 3 (c-Casp3) and cleaved PARP (c-PARP) (F). Data in A, C, D and F were expressed as mean ± SE and analyzed by two-way ANOVA (n=3-4). The *scale bars* in A and D are 500 μm. *p<0.05,** p<0.01.

Figure 5. **DOX enhanced S6K1 signaling, whereas resveratrol attenuated it**.
Cardiomyocytes were treated with resveratrol and DOX either alone or in combination for 18 hours before subjected to Western blot analysis (A). The protein levels of phosphorylated S6K1 and S6 were normalized to total S6K1 and total S6 levels, respectively, and quantified by densitometry (right panels of A). The kinase activity of S6K1 was measured by an immuno-

complex kinase assay using MBP as the substrate (B). The immunoprecipitation (IP) was performed using a S6K1 antibody. An ERK2 antibody and regular IgG served as positive and negative controls, respectively. The α1-adrenergic receptor agonist phenylephrine (PE, 25 μM) was used to stimulate ERK activity. Phosphorylated MBP on serine site was detected by immunoblot (IB) using an anti-phosphoserine antibody and quantified by densitometry assay. Data were expressed as mean ± SE and analyzed by one-way ANOVA (n=3-4). *p<0.05, **p<0.01 versus vehicle control, #p<0.05 versus DOX.

Figure 6. S6K1 knockdown attenuated DOX-induced autophagy and resveratrol failed to further reduce it. NRCs were transfected with control small interfering RNA (siCON) or siRNA against S6K1 (siS6K1) for 36 h, and then treated with DOX and resveratrol in the presence or absence of BFA. Phosphorylated and total S6K1 were analyzed following siRNA transfection (A). Autophagic activity was assessed by the protein levels of LC3-II (B) and the accumulation of autophagic vacuoles (AVs) indicated by GFP-LC3 dots (C) in the absence and presence of BFA. Autophagic flux was quantified by LC3-II levels (D) or percentage of AVs positive cells (E). Data were expressed as mean ± SE and analyzed by two-way ANOVA followed by paired student's *t* test (n=4). The *scale bar* in C is 50μm. **p<0.01.

Figure 7. S6K1 knockdown attenuated DOX-induced cardiomyocyte death, but resveratrol did not provide further protection. NRCs were transfected with siCON or siS6K1 for 36 hours, and then treated with resveratrol (10μM) and DOX (1 μM), alone or together. Cardiomyocyte death was determined by PI staining (A and B), DNA laddering (C), cleaved caspase 3 (c-Casp3) and cleaved PARP(c-PARP) (D). Data were expressed as mean ± SE and analyzed by two-way ANOVA (n=3-4). The *scale bar* in A is 500μm. *p<0.05,** p<0.01.

Figure 8. Overexpression of S6K1 abolished the ability of resveratrol to inhibit DOX-induced autophagy. NRCs were infected with Adβgal or AdS6K1 at indicated MOI for 36h, and

P70S6K and the phosphorylation of its downstream target ribosome S6 were analyzed with Western blotting (A). After adenoviral infection, cardiomyocytes were treated with resveratrol for 12 hours before exposed to DOX for another 18 h. Autophagic activity was assessed by either LC3-II protein levels (B) or GFP-LC3 dots (C) in the presence or absence of BFA. Autophagic flux was quantified by relative LC3II levels (D) or AV positive cells (E). Data were expressed as mean ± SE and analyzed by two-way ANOVA followed by paired student's *t* test (n=3). The *scale bar* in C is 50μm. ** p<0.01.

Figure 9. Overexpression of S6K1 impaired the ability of resveratrol to antagonize DOX-induced cardiomyocyte death. NRCs were infected with Adβgal or AdS6K1 for 24 h, and treated with 10 μM resveratrol for 12 h before exposed to 1μM DOX. Cell death was determined by PI staining (A and B), Western blot analysis of cleaved caspase3 (c-Casp3) and cleaved PARP(c-PARP) (C) and DNA laddering (D). Data were expressed as mean ± SE and analyzed by two-way ANOVA (n=4). The *scale bar* in A is 500 μm. *p<0.05,** p<0.01.

Figure 1

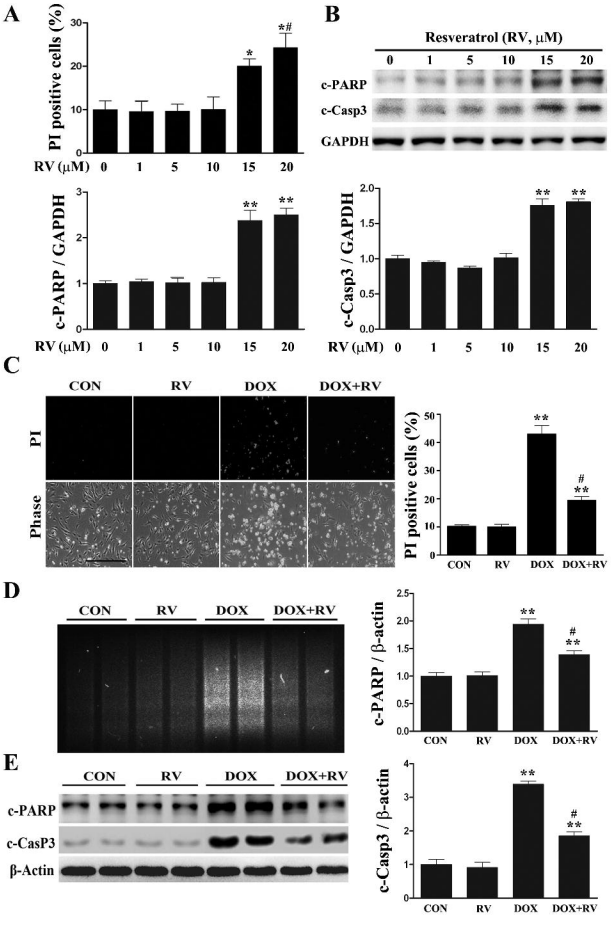
A
PI positive cells (%)
RV (μM) 0 1 5 10 15 20
c-PARP / GAPDH
c-Casp3 / GAPDH
B
Resveratrol (RV, μM)
0 1 5 10 15 20
c-PARP
c-Casp3
GAPDH
C
CON
RV
DOX
DOX+RV
PI
Phase
PI positive cells (%)
D
c-PARP / β-actin
E
c-PARP
c-CasP3
β-Actin
c-Casp3 / β-actin

Figure 2

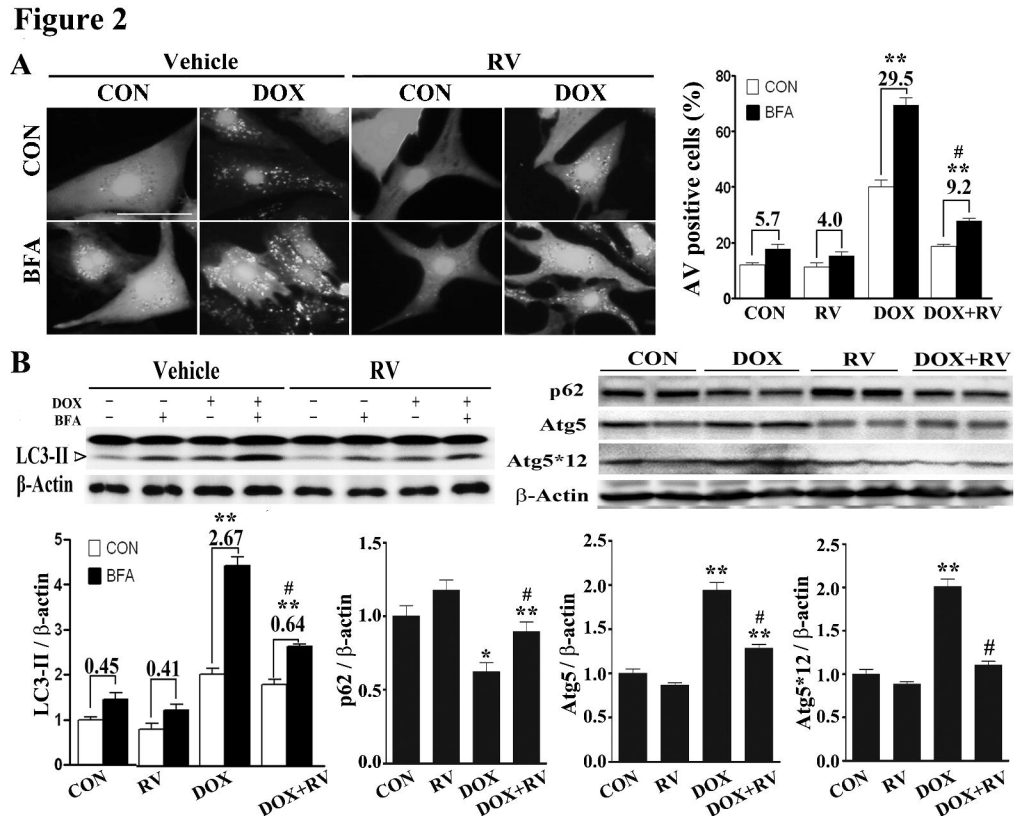
A
Vehicle
RV
CON
DOX
CON
DOX
CON
BFA
AV positive cells (%)
CON
BFA
5.7
4.0
**
29.5
#
**
9.2
CON
RV
DOX
DOX+RV
B
Vehicle
RV
DOX
BFA
LC3-II
β-Actin
CON
DOX
RV
DOX+RV
p62
Atg5
Atg5*12
β-Actin
LC3-II / β-actin
0.45
0.41
**
2.67
#
**
0.64
p62 / β-actin
Atg5 / β-actin
Atg5*12 / β-actin
CON
RV
DOX
DOX+RV

Figure 3

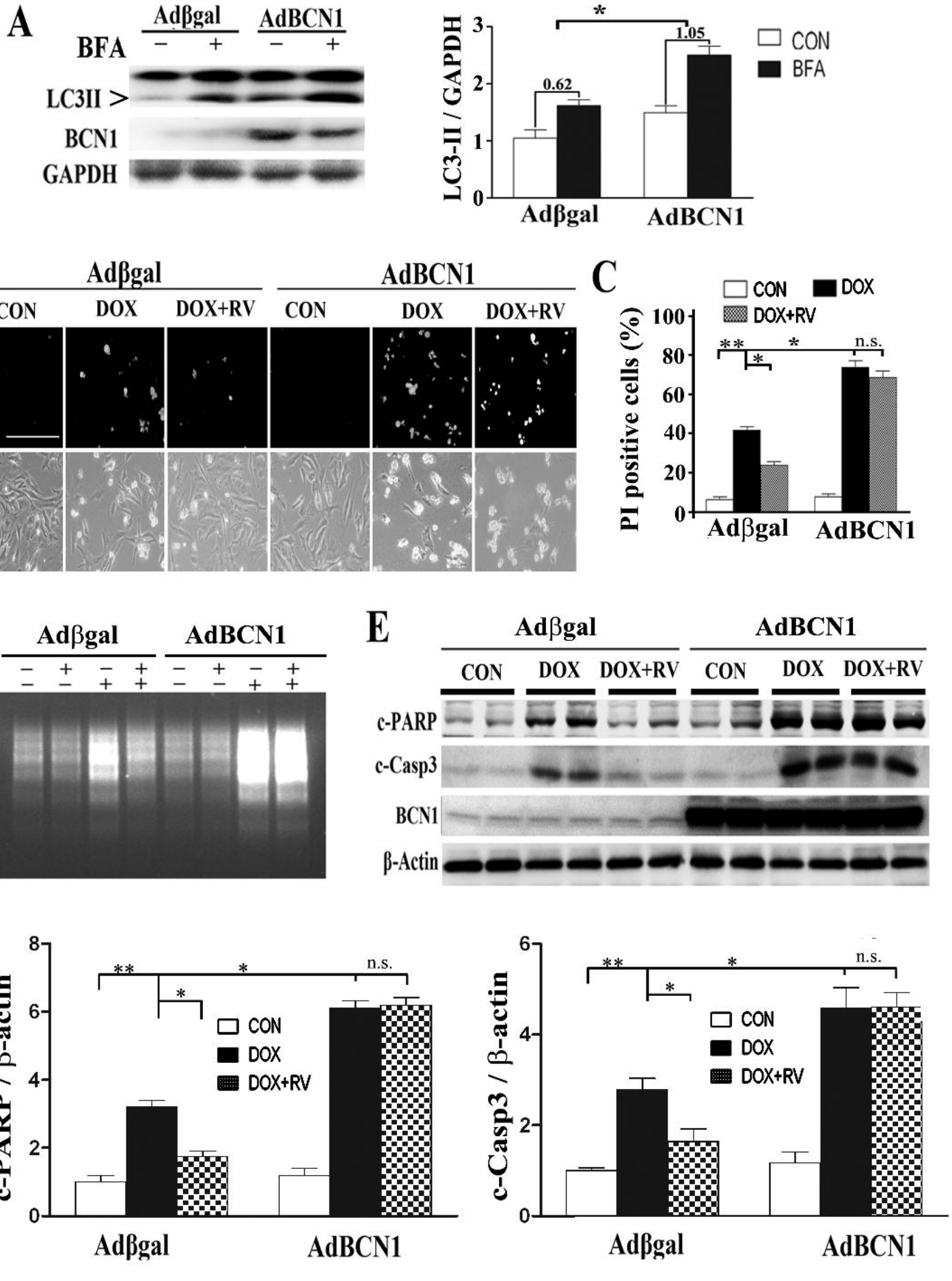
A
Adβgal
AdBCN1
BFA
− + − +
LC3II
BCN1
GAPDH
LC3-II / GAPDH
0.62
1.05
CON
BFA
Adβgal
AdBCN1
B
Adβgal
AdBCN1
CON
DOX
DOX+RV
PI
Phase
C
CON
DOX
DOX+RV
PI positive cells (%)
n.s.
D
RV
DOX
DNA laddering
E
c-PARP
c-Casp3
BCN1
β-Actin
c-PARP / β-actin
c-Casp3 / β-actin

Figure 4

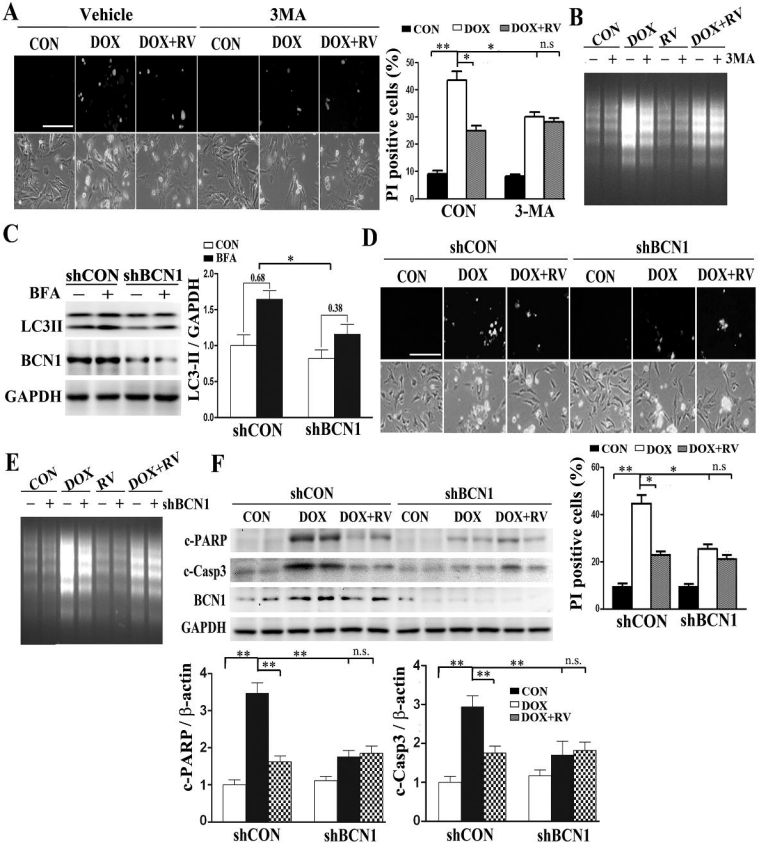
A
Vehicle
3MA
CON
DOX
DOX+RV
CON
DOX
DOX+RV
CON
DOX
DOX+RV
PI positive cells (%)
CON
3-MA
B
CON
DOX
RV
DOX+RV
3MA
C
shCON
shBCN1
BFA
LC3II
BCN1
GAPDH
CON
BFA
LC3-II / GAPDH
0.68
0.38
shCON
shBCN1
D
shCON
shBCN1
CON
DOX
DOX+RV
CON
DOX
DOX+RV
E
CON
DOX
RV
DOX+RV
shBCN1
F
shCON
shBCN1
CON
DOX
DOX+RV
CON
DOX
DOX+RV
c-PARP
c-Casp3
BCN1
GAPDH
CON
DOX
DOX+RV
PI positive cells (%)
shCON
shBCN1
c-PARP / β-actin
c-Casp3 / β-actin
CON
DOX
DOX+RV
shCON
shBCN1
shCON
shBCN1

Figure 5

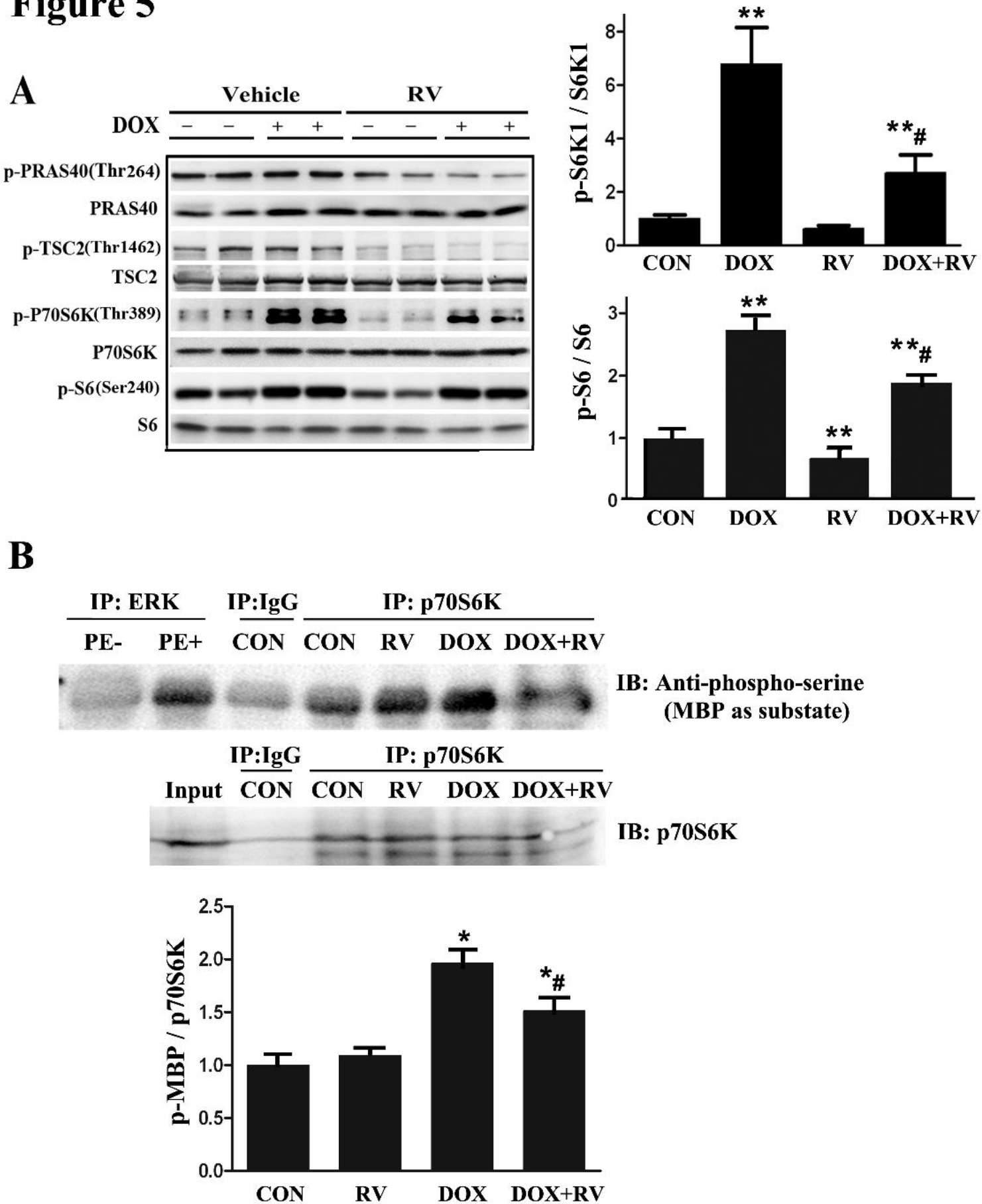
A
Vehicle
RV
DOX
– – + + – – + +
p-PRAS40(Thr264)
PRAS40
p-TSC2(Thr1462)
TSC2
p-P70S6K(Thr389)
P70S6K
p-S6(Ser240)
S6
p-S6K1 / S6K1
**
**#
CON
DOX
RV
DOX+RV
p-S6 / S6
**
**
**#
CON
DOX
RV
DOX+RV
B
IP: ERK
IP:IgG
IP: p70S6K
PE-
PE+
CON
CON
RV
DOX
DOX+RV
IB: Anti-phospho-serine
(MBP as substate)
IP:IgG
IP: p70S6K
Input
CON
CON
RV
DOX
DOX+RV
IB: p70S6K
p-MBP / p70S6K
*
*#
CON
RV
DOX
DOX+RV

Figure 6

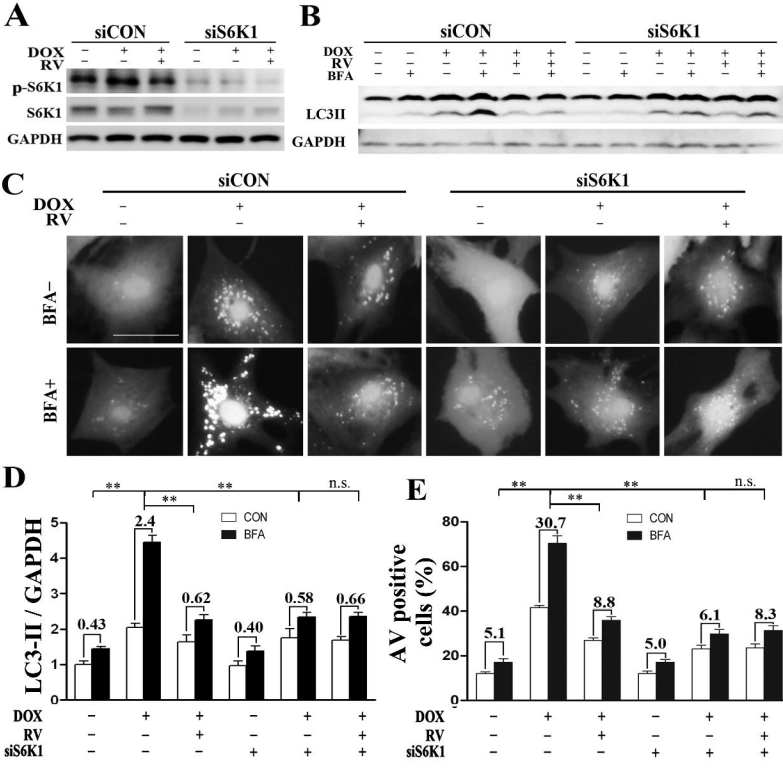
A
siCON
siS6K1
DOX
RV
p-S6K1
S6K1
GAPDH
B
siCON
siS6K1
DOX
RV
BFA
LC3II
GAPDH
C
siCON
siS6K1
DOX
RV
BFA−
BFA+
D
LC3-II / GAPDH
CON
BFA
0.43
2.4
0.62
0.40
0.58
0.66
**
**
**
n.s.
DOX
RV
siS6K1
E
AV positive cells (%)
CON
BFA
5.1
30.7
8.8
5.0
6.1
8.3
**
**
**
n.s.
DOX
RV
siS6K1

Figure 7

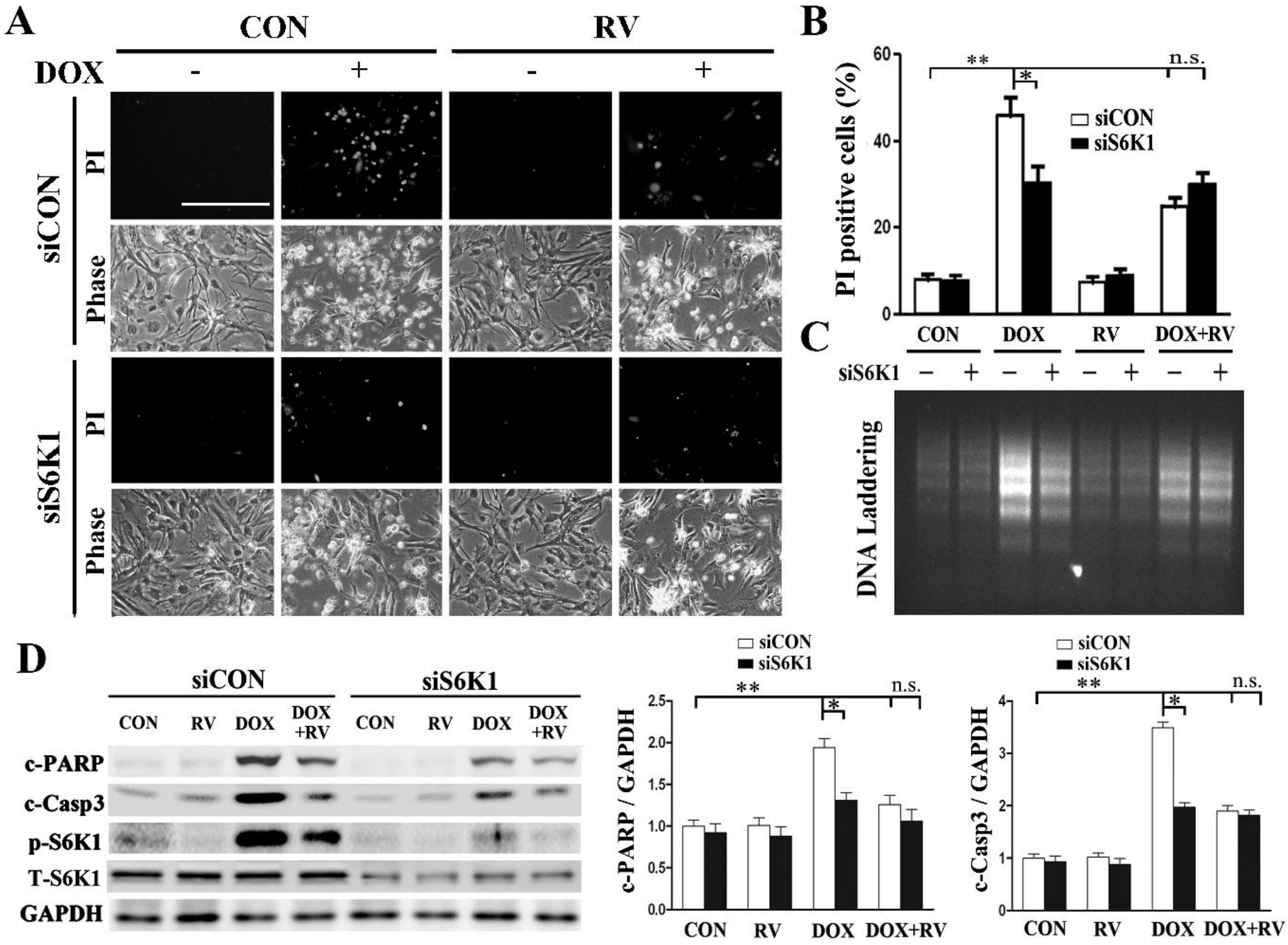
A
CON
RV
DOX
-
+
-
+
siCON
siS6K1
PI
Phase
B
PI positive cells (%)
60
40
20
0
**
*
n.s.
siCON
siS6K1
CON
DOX
RV
DOX+RV
C
siS6K1
DNA Laddering
D
siCON
siS6K1
CON
RV
DOX
DOX +RV
c-PARP
c-Casp3
p-S6K1
T-S6K1
GAPDH
c-PARP / GAPDH
c-Casp3 / GAPDH

Figure 8

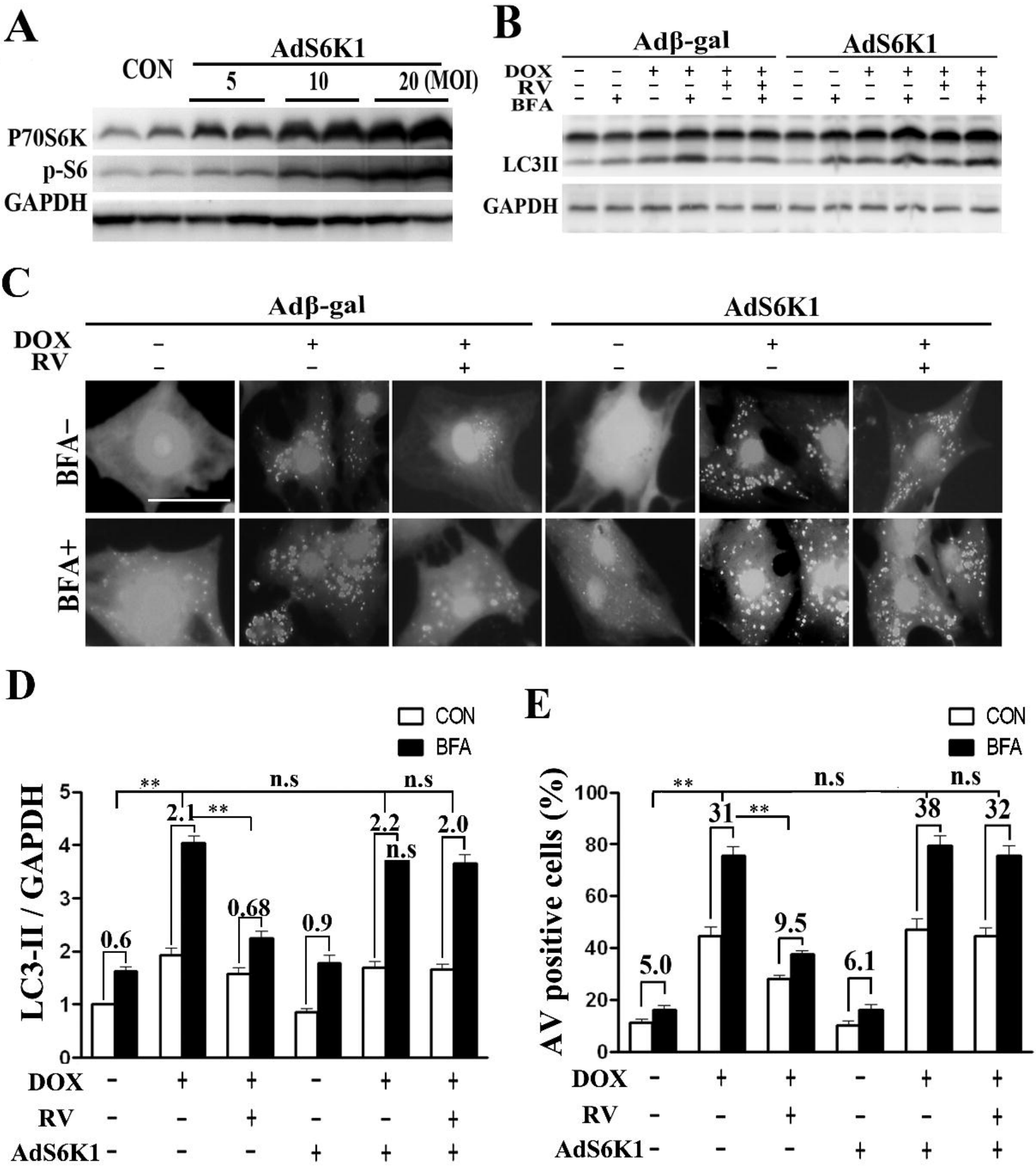
A
CON
AdS6K1
5
10
20 (MOI)
P70S6K
p-S6
GAPDH
B
Adβ-gal
AdS6K1
DOX
RV
BFA
LC3II
GAPDH
C
Adβ-gal
AdS6K1
DOX
RV
BFA−
BFA+
D
CON
BFA
LC3-II / GAPDH
**
n.s
n.s
2.1
**
2.2
n.s
2.0
0.6
0.68
0.9
DOX
RV
AdS6K1
E
CON
BFA
AV positive cells (%)
**
n.s
n.s
31
**
38
32
5.0
9.5
6.1
DOX
RV
AdS6K1

Figure 9

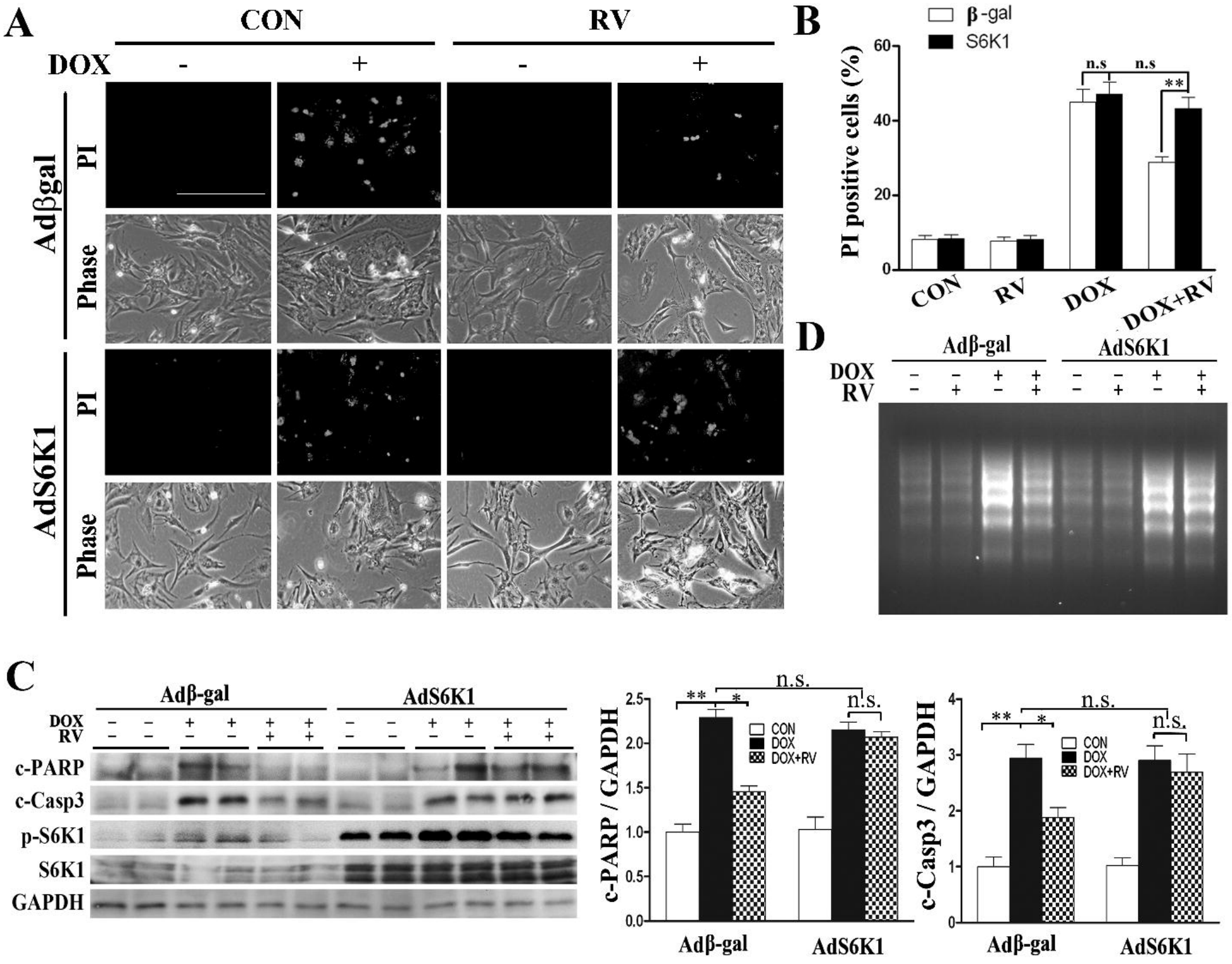
A
CON
RV
DOX
-
+
-
+
AdβgalPI
Phase
AdS6K1
PI
Phase
B
β-gal
S6K1
PI positive cells (%)
60
40
20
0
n.s
n.s
**
CON
RV
DOX
DOX+RV
D
Adβ-gal
AdS6K1
DOX
RV
C
Adβ-gal
AdS6K1
DOX
RV
c-PARP
c-Casp3
p-S6K1
S6K1
GAPDH
c-PARP / GAPDH
2.5
2.0
1.5
1.0
0.5
0.0
**
*
n.s.
n.s.
CON
DOX
DOX+RV
Adβ-gal
AdS6K1
c-Casp3 / GAPDH
4
3
2
1
0
**
*
n.s.
n.s.
CON
DOX
DOX+RV
Adβ-gal
AdS6K1